# Strip Detectors Processed on High-Resistivity 6-inch Diameter Magnetic Czochralski Silicon (MCz-Si) Substrates

X. Wu, J. Härkönen, J. Kalliopuska, E. Tuominen, T. Mäenpää, P. Luukka, E. Tuovinen, A. Karadzhinova, L. Spiegel, S. Eränen, A. Oja, and A. Haapalinna

***Abstract*—Tracking detectors for future high-luminosity particle physics experiments have to be simultaneously radiation hard and cost efficient. This paper describes processing and characterization of $p^+/n^-/n^+$ (n-type silicon bulk) detectors made of high-resistivity Magnetic Czochralski silicon (MCz-Si) substrates with 6-inch wafer diameter. The processing was carried out on a line used for large-scale production of sensors using standard fabrication methods, such as implanting polysilicon resistors to bias individual sensor strips. Special care was taken to avoid the creation of Thermal Donors (TD) during processing. The sensors have a full depletion voltage of 120-150 V which are uniform over the investigated sensors. All of the leakage current densities were below $55\ nA/cm^2$ at 200 V bias voltage. A strip sensor with 768 channels was attached to readout electronics and tested in particle beam with a data acquisition (DAQ) similar to the system used by the CMS experiment at the CERN LHC. The test beam results show a signal-to-noise ratio greater than 40 for the test beam sensor. The results demonstrate that MCz-Si detectors can reliably be manufactured in the industrial scale semiconductor process.**

***Index Terms*—High energy physics, radiation hardness, silicon radiation sensors, strip detector.**

## I. Introduction

THE performance of the CERN Large Hadron Collider (LHC) is gradually improving, enabling new particle physics discoveries. A major accelerator upgrade, boosting the luminosity by an order of magnitude, is planned to take place after about ten years of operation [1]. The concept known as high-luminosity LHC (HL-LHC) would result in an integrated fast hadron fluence of $1.5 \times 10^{15}$ neq/cm$^2$ (1 MeV neutron equivalent fluence) for the innermost strip layers and about $1 \times 10^{16}$ neq/cm$^2$ for the pixel layers in the silicon tracking systems [2], [3]. The most important measure of the detector radiation hardness is the Charge Collection Efficiency (CCE), which is mainly affected by the electric field distribution in the irradiated silicon, and the charge trapping by radiation-induced centers. At the expected maximum fluence of the strip sensor layers, the required full depletion voltage ($V_{fd}$) would be on the scale of thousand volts for a 300 $\mu$m thick oxygen-lean Float Zone silicon (Fz-Si) [4], [5], [6]. Moreover, when heavily irradiated the Fz-Si undergoes Space Charge Sign Inversion (SCSI) in which the maximum electric field shifts from the segmented front side towards the back plane of the $p^+/n^-/n^+$ (p on n, or n-type sensor) structured sensor. Thus, SCSI together with significant trapping makes traditional n-type Fz-Si strip sensors unusable in the high-luminosity environment [7].

Improving the radiation hardness of silicon detectors has been of interest in the scientific community for the past couple of decades. The CERN RD48 Collaboration reported diffusion oxygenation of Fz-Si to result in a lower increase of $V_{fd}$ compared with the oxygen-free silicon materials when irradiated with charged particles. Very little or no effect of oxygenation had been observed when irradiated with neutrons [8]. RD48 developments were followed by the RD50 proposals for using naturally oxygen-rich high-resistivity Czochralski silicon (Cz-Si or MCz-Si if grown in a magnetic field) [9], [10] and device engineering in terms of $n^+/p^-/p^+$ (n on p, or p-type sensor) structure [11], [12], [13]. P-type detectors do not suffer from SCSI and thus the electric field maximum remains on the segmented side of the sensor. CCE is further enhanced by the Weighting Field (WF) effect [14], [15], which is based on the electrostatic coupling between the drifting charge and the sensing electrode. Thus, if a high electric field E(x) is present at the segmented side of a position sensitive detector, the CCE is largely increased.

The drawback of p-type devices is the more complex fabrication technology. This is due to the positive oxide charge of the dielectric layers on the detector. There are basically two methods to suppress the electron accumulation near the surface: p-spray and p-stop techniques. The p-spray method utilizes boron field implantation, which provides positive space charge

Manuscript received February 12, 2013; revised May 30, 2013; accepted December 14, 2013. Date of current version February 06, 2014. This work was supported in part by the Academy of Finland, VTT Graduate School and High-Performance-Microsystem Innovation Program of VTT.

X. Wu, J. Kalliopuska, S. Eränen, and A. Oja are with the VTT Technical Research Center of Finland, FI-02044 Espoo, Finland (e-mail: xiaopeng.wu@vtt.fi; juha.kalliopuska@vtt.fi; simo.eranen@vtt.fi; aarne.oja@vtt.fi).

J. Härkönen, E. Tuominen, T. Mäenpää, P. Luukka, E. Tuovinen, and A. Karadzhinova are with the Helsinki Institute of Physics, CMS Upgrade Project, Gustaf Hällströmin katu, University of Helsinki, 00100 Helsinki, Finland (e-mail: jaakko.haerkoenen@cern.ch; eija.tuominen@helsinki.fi; teppo.maenpaa@cern.ch; panja.luukka@cern.ch; esa.tuovinen@helsinki.fi; aneliya.karadzhinova@helsinki.fi).

L. Spiegel is with Fermi National Accelerator Laboratory, Batavia, IL 60510 USA (e-mail: lenny@fnal.gov).

A. Haapalinna is with Okmetic Oyj, Piitie 2, FI-01510 Vantaa, Finland (e-mail: atte.haapalinna@okmetic.com).

Color versions of one or more of the figures in this paper are available online at http://ieeexplore.ieee.org.

Digital Object Identifier 10.1109/TNS.2013.2295430

0018-9499 © 2014 IEEE. Translations and content mining are permitted for academic research only. Personal use is also permitted, but republication/redistribution requires IEEE permission. See http://www.ieee.org/publications_standards/publications/rights/index.html for more information.

near the surface and thus compensates the electron accumulation. The p-stop method involves a localized $\mathrm{p}^+$ implant that terminates the surface inversion. Both methods, however, involve increased process complexity and, in addition, might lead to localized high electric fields, which increase the likelihood of early breakdowns [16].

During the past ten years, detectors made of high-resistivity Cz-Si and MCz-Si materials have been subjected to many studies [17], [18], [19], including electric field distribution analysis with the Transient Current Technique (TCT) method [20], [21], [22], [23] and test beam measurements of full-size strip detectors [24]. Test beam measurements performed with CMS front-end electronics and data acquisition (DAQ) on MCz-Si detector irradiated to $1.1 \times 10^{15}$ neq/cm$^2$ fluence revealed a 50% CCE and a signal-to-noise (SNR) ratio of more than ten. The finding was supported by TCT measurements, which showed a double-peak for the electric field distribution E(x) in MCz-Si sensors, suggesting that the electric field on the segmented side remaining strong even after heavy irradiation [25], [26], [27].

In this context, we report the successful processing and characterization of MCz-Si detectors made on 150 mm diameter wafers manufactured on a fully automated, cassette-to-cassette industrial process line capable of annual production of thousands of silicon wafers. It is worth noting that the capability to use 150 mm wafers instead of 100 mm wafers is essential since the modern semiconductor processing equipment is designed for larger wafer sizes and the 100 mm wafers are becoming difficult to obtain due to the limited demands. Since the MCz-Si intrinsically contains oxygen, we have put special emphasis to avoid the formation of thermal donors.

## II. Processing of MCz-Si Detector

The 150 mm diameter n-type MCz silicon wafers with crystal orientation of $< 100 >$ were provided by Okmetic Ltd. The nominal thickness of the single-sided polished wafers is $330\ \mu$m and the average resistivity mapped with four-point probe (4PP) was about 2000 Ohm $\cdot$ cm. The interstitial oxygen concentration was measured, using the Fourier Transform Infrared Spectroscopy method defined in the standard ASTM F1188-93a [28], to be homogeneously $2.9 - 3.0 \times 10^{17}$ cm$^{-3}$.

The charge carrier recombination lifetime in the silicon substrates was studied by using $\mu$PCD (Microwave detected Photoconductive Decay) method [29], [30]. The recombination lifetime is a measure of the material quality i.e., the defect and impurity concentration that affects the quality of the detectors and their electrical properties. The lifetimes were mapped by Semilab WT85 scanning tool with a 2 mm $\times$ 2 mm raster, resulting in about 1800 data points. The measurements were carried out at high injection level, i.e. laser pulse excitation is much larger than the free carrier concentration caused by the doping. The measured wafers were passivated by thermally oxidized dry silicon dioxide. The histogram of lifetime data points is shown in Fig. 1.

The average value of lifetime is $3070\ \mu$s and it can be seen that after about $3300\ \mu$s the numbers of entries falls off and there are no entries above $3400\ \mu$s. This is because the measured lifetime, often called as effective lifetime, is a complex combination of surface recombination velocity and carrier recombination lifetime in the silicon bulk. In this case, with the given wafer thickness and surface recombination, it is impossible to measure effective lifetimes higher than $3400\ \mu$s due to the surface contribution. The lifetime measurement proves that the MCz-Si material is as good as Fz-Si. In addition, the $\mu$PCD measurement does not show any localized contamination which is especially important for large area devices.

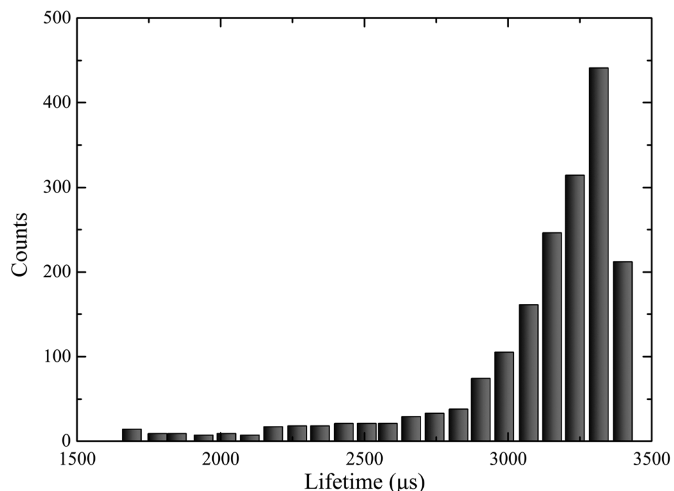


Fig. 1. Histogram of about 1800 lifetime measurement data points mapped over a thermally dry oxidized process monitor wafer.

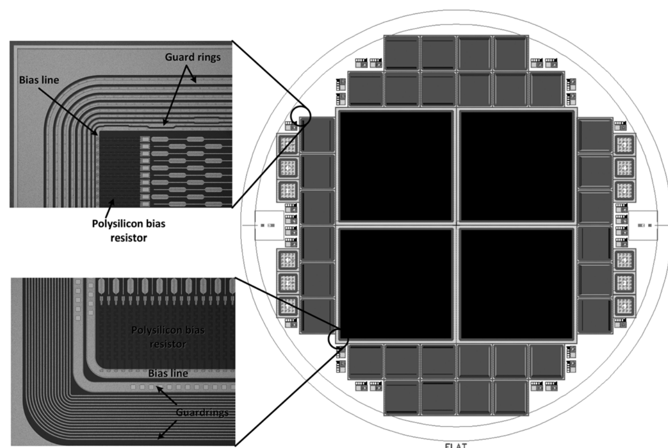


Fig. 2. The layout of the 6-inch wafer. The two insets on the left show the corners of AC-coupled strip detectors. All strips have $10\ \mu$m width but strip pitch varies from $50\ \mu$m to $80\ \mu$m in different sensors. Strip electrodes are connected to a common bias ring through serpentine-layout polysilicon resistors. In the mini-strip sensors, the active areas are embraced by 6 guard rings with stepup pitches, while in the full-size strip sensors, 16 isometric narrow guard rings and one wide guard ring are implemented.

The layouts used for the 6-inch wafer process were provided by the Helsinki Institute of Physics. The wafer contains four $3.87 \times 3.76$ cm$^2$ AC-coupled strip detectors, thirty-two $1 \times 1$ cm$^2$ AC-coupled mini-strip detectors and twenty-eight $0.5 \times 0.5$ cm$^2$ diodes. Fig. 2 shows the 6-inch wafer layout and design details of the AC-coupled strip detector.

The wafer processing was performed at the Microelectronic Center of VTT (Technical Research Center of Finland). VTT has all equipment necessary for 150 mm wafer fabrication. Totally six MCz-Si wafers and two monitoring Fz-Si wafers were

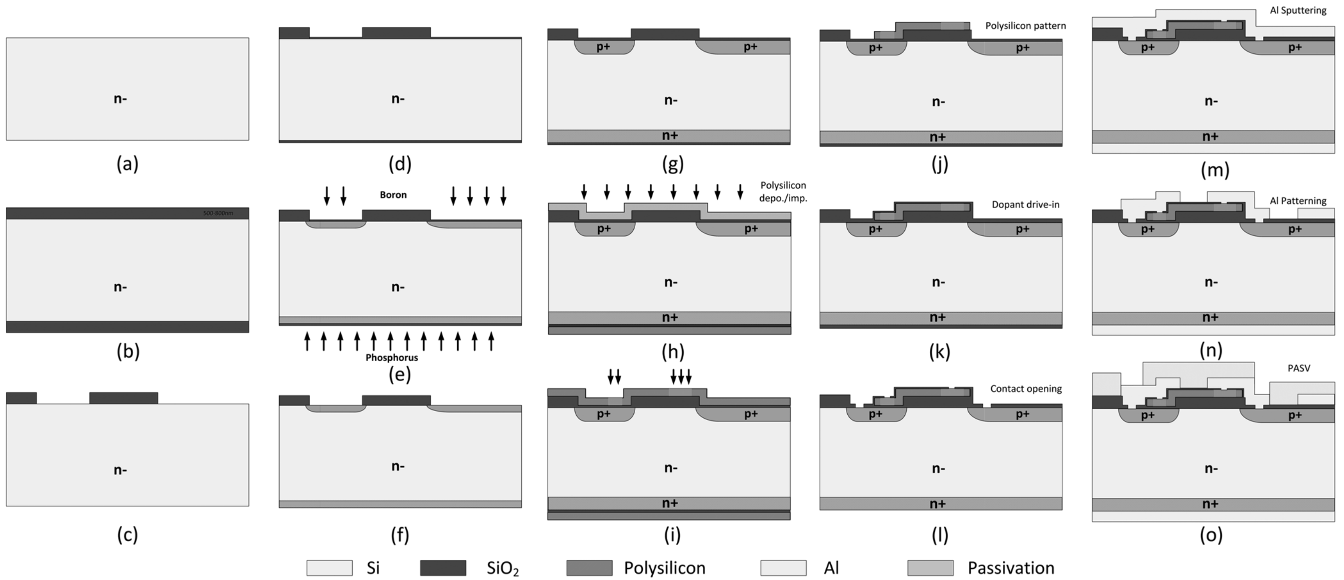


Fig. 3. Process sequence illustration of MCz-Si detectors.

processed. A brief description of the process is graphically represented in Fig. 3. Frequently repeated routine steps such as wafer cleaning, photoresist depositions and strippings are excluded.

The starting wafers (a) were thermally wet oxidized at 950 °C (b). Implantation windows were opened in the masking field oxide layer (c) and followed by the growth of a 70 nm screen oxide layer at 950 °C (d). Blank boron and phosphorous implantations were made on two sides of the wafer respectively through the screen oxide layer (e). After removing the damaged screen oxide layer (f), a 100 nm silicon dioxide layer was grown at 1050 °C as the strip coupling insulator (g). The implanted ions were simultaneously activated. A 500 nm polysilicon layer was deposited by LPCVD (Low Pressure Chemical Vapor Deposition) technology. The polysilicon layer was implanted with boron ions to adjust the target resistivity (h). An extra implantation with the high dose was then given to defined regions of polysilicon to achieve the low contact resistance between polysilicon and strip implants (i). After the reactive ion etching of polysilicon (j), the implanted ions in polysilicon were activated during a subsequent dry oxidation at 950 °C resulting in simultaneously designed strip insulator thickness of 150 nm (k). Contact windows were opened on polysilicon resistors and on desired regions on $p^+$ implants (l). Aluminum layers of 1 $\mu$m were sputtered on both sides of the wafer (m). The front side metal was patterned (n). The processing was ended with the Plasma-enhanced Chemical Vapor Deposition (PECVD) of the $SiO_2$ passivation at 300 °C followed by a furnace annealing at 350 °C in the forming gas ambient (o).

It is well known that the aggregation of oxygen atoms leads to a formation of electrically active defects, commonly referred to as the thermal donors (TDs). When processing n-type ($p^+$ segmentation on phosphorous doped bulk) MCz-Si detectors, the TD formation is generally harmful. TDs result in additional donor doping of the bulk and thus elevate the $V_{fd}$. The formation of TDs starts approximately at an annealing temperature of 400 °C and annihilation will take place at temperatures above 600 °C [31], [32], [33], [34], [35], [36]. Thus, temperatures in the range of 400-600 °C were avoided after the last high temperature process step.

The special emphasis was put on the last high temperature processes, namely dry oxidation at 950 °C (Fig. 3, k), PECVD (between n and o) and the annealing process (after o). In the dry oxidation process, it is of utmost importance to correctly finish the processing step. We used loading and unloading temperature of 700 °C. According to our previous studies [36], we estimate that after the oxidation the sample stays at temperature of 400 - 600 °C only in a very short time. This, however, does generate some TDs but not enough to remarkably affect the bulk resistivity and the detector behavior. On the other hand, it is of utmost importance to perform the PECVD and annealing in temperatures well below 400 °C, in our case 300 °C and 350 °C, respectively.

## III. Electrical Characterization

Electrical characterization was performed on the large $3.87 \times 3.76$ cm$^2$ strip sensors, $1 \times 1$ cm$^2$ mini-sensors, and $0.5 \times 0.5$ cm$^2$ diodes using a probe station in a dark chamber. The dimensions refer to active areas enclosed by the guard rings, which are grounded during the measurements. The Capacitance-Voltage (C-V) measurement was performed with an Agilent 4263B LCR meter with a 10 kHz 500 mV signal superimposed on a DC level. Previous measurements of the open loop capacitance, including the capacitance induced by the AC-coupling of the high voltage bias, were subtracted from the measurement data. Fig. 4 shows C-V curves of mini-sensors. Totally three processed MCz-Si wafers were investigated and the data points and error bars were constructed from 20 C-V measurements on each wafer. The y-axis error bars are standard deviations of the average values.

The depletion voltages were determined from the plots of $1/C^2$ vs. bias voltage. When a detector is fully depleted, the measured capacitance value does not decrease anymore and saturates on the value $C = \varepsilon_{Si}{}^*\varepsilon_0{}^*(A/t)$, where $\varepsilon_{Si}$ is permittivity in silicon, $\varepsilon_0$ permittivity in vacuum, A detector area, and

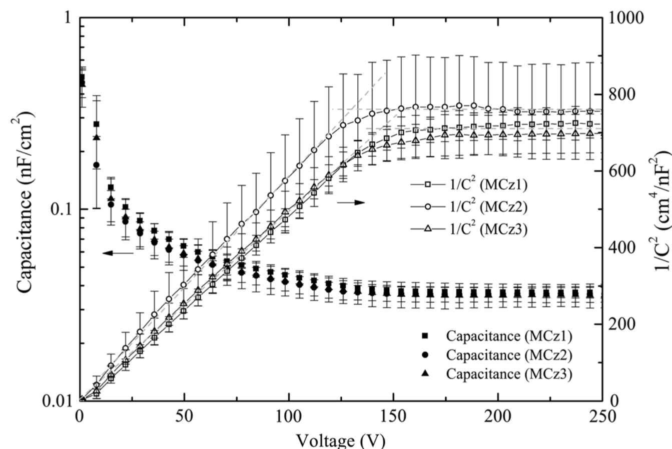


Fig. 4. C-V curves of 1 cm$^2$ mini-sensors. The measurement was performed on three wafers and 20 mini-sensors were measured on each wafer. The Vfd is extracted from the intersection of two fitting lines of the $1/\mathrm{C}^2$ vs. voltage curves.

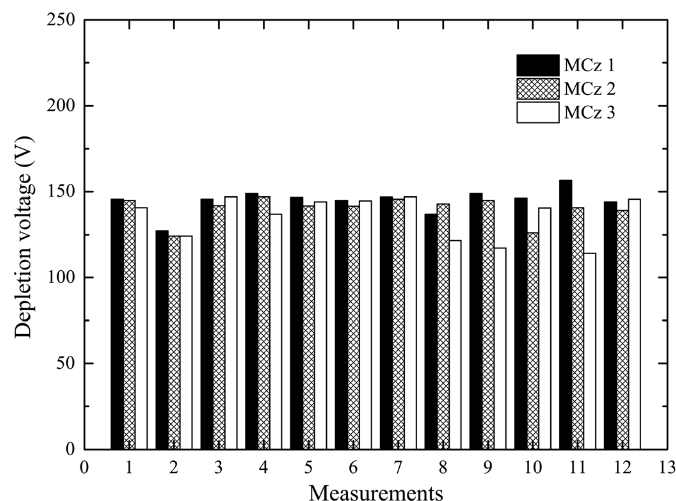


Fig. 5. Depletion voltages extracted from 12 C-V measurements of the mini-strip sensors on three process wafers. Sample numbers are arbitrary.

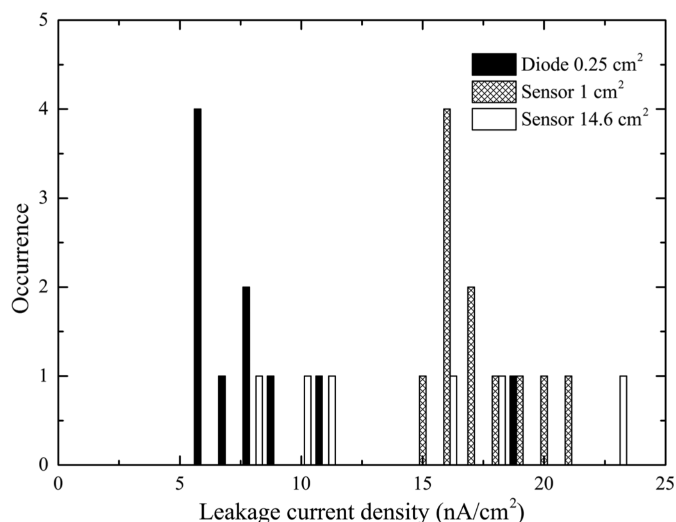


Fig. 6. Histogram of leakage current density at 200 V reverse bias. The measurement was performed at room temperature.

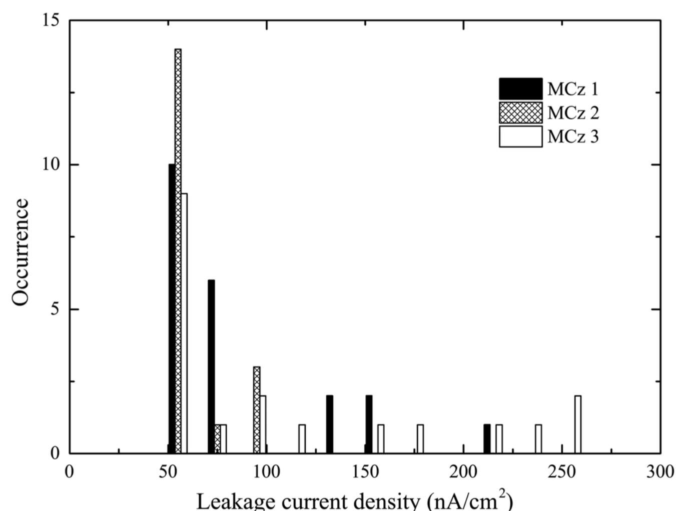


Fig. 7. Leakage current densities measured from the mini-sensors of three process wafers. The measurement was performed at room temperature.

t detector thickness. Before full depletion, the $1/\mathrm{C}^2$ term can be expressed as a function of the bias voltage V : $1/\mathrm{C}^2 = 2/(\mathrm{q}^*\varepsilon_{\mathrm{Si}}{}^*\varepsilon_0{}^*\mathrm{N}^*\mathrm{A}^2)^*\mathrm{V}$, where N is the doping density. Thus the depletion voltage can be extracted by fitting two first order polynomials to the $1/\mathrm{C}^2$ vs. voltage graph and calculating the intersection points, as shown in Fig. 4.

The resistivity of MCz-Si wafers were measured prior the processing by four-point-probe method resulting in a value of about 2 kOhm $\cdot$ cm, which would correspond the depletion voltage of about 180 V. The $\mathrm{V}_{\mathrm{fd}}$ of the processed sensors, measured by probe station from more than 50 samples from several wafers, vary within 120 - 150 V, corresponding to $2.5 - 2.9$ Ohm $\cdot$ cm. It is worth noting that this is the first time when MCz-Si detectors were manufactured resulting in the after-process resistivity of this scale. However, we think that the apparent increase in resistivity after processing is best explained by the inaccuracy of four-point probe method, used on non-processed wafers. The 4PP is commonly used in CMOS applications, i.e. to measure the resistivity in the range of $1 - 10$ Ohm $\cdot$ cm, or sheet resistivity of metallic thin films, but not of high resistivity materials. 4PP systems use tungsten prone needles, which do not necessarily contact well with $> 1$ kOhm $\cdot$ cm bare silicon surface.

The specific capacitances at 250 V for the investigated mini-sensors on the three wafers are $37.2 \pm 0.9$, $36.7 \pm 2.6$ and $37.9 \pm 1.3$ pF/cm$^2$ respectively. Fig. 5 shows the depletion voltages extracted from 12 C-V measurements of the mini-strip sensors originally situating at the different edges of the silicon wafer. The depletion voltages are 120-150 V and uniform over the investigated sensors from different wafers.

During the Current-Voltage (I-V) measurement, the bias voltage was fed from the backside of the chip and current was read from the common bias line while the innermost guard ring was kept at the ground potential. A summary of the leakage current measurements is given in Fig. 6. The leakage current of mini-sensors measured from the three wafers is shown in Fig. 7. In all the wafers, most of the leakage currents fall into the range of $0 \sim 55$ nA/cm$^2$.

The polysilicon resistance was monitored during the process and in the characterization phase. The process monitor wafers were oxidized blank wafers with 500 nm of polysilicon on top

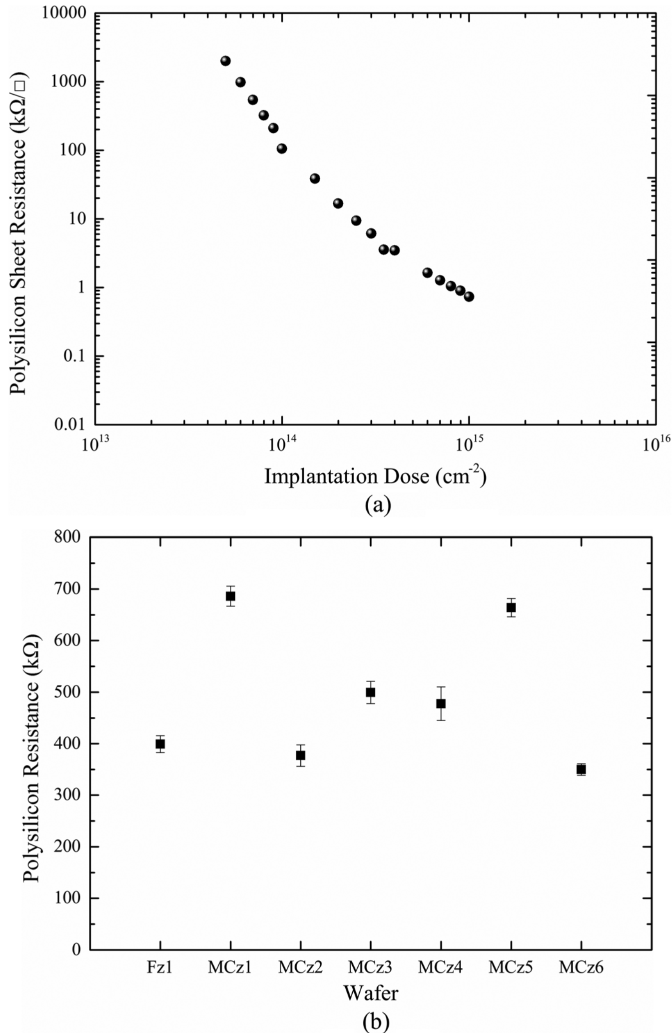


Fig. 8. The poly-silicon resistance monitored on (a) the monitor wafers and (b) the process wafers.

of the oxide layer. Wafers were sent for implantation with various doses at a constant energy of 30 keV. The polysilicon sheet resistance was measured using a four-probe method and the results, shown in Fig. 8(a), can be used to find the proper implantation parameters in the process. Fig. 8(b) shows the values of polysilicon resistors on all process wafers. Most of the resistances fall in the 350 to 500 kOhm range. The wafers MCz1 and MCz5 were not passivated when the measurement was performed, which might explain why they have a larger variation than the others.

## IV. Test Beam Results

The motivation of the test beam measurements is to demonstrate that the industrially processed position-sensitive MCz-Si detectors are able to fulfill their purpose, i.e. track particles with sufficient signal-to-noise ratio and resolution, resulting in trustworthy particle tracking and identification.

One $3.87 \times 3.76$ cm$^2$ sensor with 50 $\mu$m strip pitch and 768 channels was selected for a test beam measurement. The full depletion voltage for this sensor was about 120 V and the leakage current from the guard ring limited area was 120 nA at $V_{fd}$ and 290 nA at 300 V. The capacitance for the area delimited

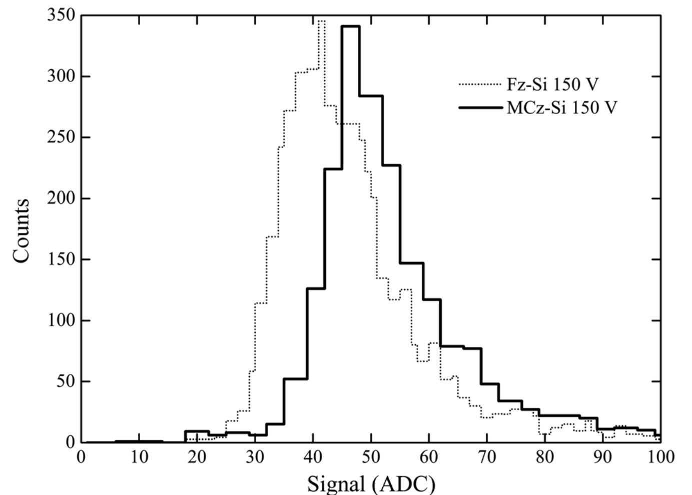


Fig. 9. Signal distributions of MCz-Si sensor under investigation and one of the telescope reference planes. The distributions consist of about 2000 reconstructed events (data run 4926) seen by all planes of the telescope. One ADC count corresponds to about 600 e$^-$ (0.1 fC) charge.

by the guard ring was 470 pF at 120 V. The sensor was first glued on a supporting PCB and then wire bonded to a CMS APV25 read-out board [37] using a pitch adapter (aluminum traces on a glass substrate) fabricated at the Micronova Centre. After the module assembly, the leakage current was measured from the bias rails of the supporting PCB resulting in 220 nA at 120 V and 300 nA at 300 V. The physical thickness of the sensor was measured with a micrometer to be 330 $\mu$m. C-V measurements made on diodes with 0.5 cm $\times$ 0.5 cm area, limited by a grounded guard ring, resulted in capacitances of 8.2 pF, which corresponds to the effective sensor thickness (fraction of silicon thickness where electric field enables charge drift transportation) of about 315 $\mu$m.

The test beam experiment was carried out in May 2012 at the CERN H2 beam line utilizing a 220 GeV muon beam from the SPS accelerator. A beam telescope, consisting of 8 reference detectors inside a Peltier cooled box [38], [39], was used to track particles passing through the DUTs. The reference detector modules are made of Fz-Si strip sensors produced by Hamamatsu Photonics K.K (HPK) for the D0 experiment at Fermi National Accelerator Laboratory (FNAL). The full depletion voltage of the reference detectors is about 100 V extracted from C-V measurements. The capacitance measured from the sensor active area (9.8 cm $\times$ 3.8 cm) is 1.38 nF corresponding to the effective thickness of about 290 $\mu$m. The physical thickness of the reference detectors is 320 $\mu$m $\pm$ 20 $\mu$m as reported with other technical details in [40]. During the data taking the reference detectors were biased with 150 V.

The data acquisition (DAQ) and off-line analysis of the telescope are based on the CMS experiment software and analysis framework [41]. The output of the DAQ is expressed in analog to digital converter (ADC) counts. For the conversion from ADC units to electric charge we assume that the reference planes operate with 100% relative CCE and the most probable value of the collected charge is on average $40 \pm 0.8$ ADC counts. Thus, taking into account minimum ionizing particle ionization in silicon (80 electron/hole pairs per micron), one ADC count corresponds to about 600 e$^-$ (0.1 fC) charge. Fig. 9 shows

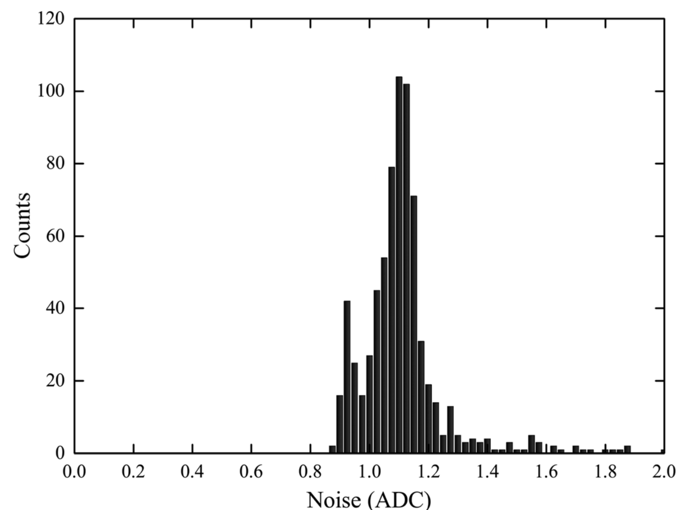


Fig. 10. The strip noise distribution for the MCz-Si detector used in the test beam. The data was recorded during run 4926.

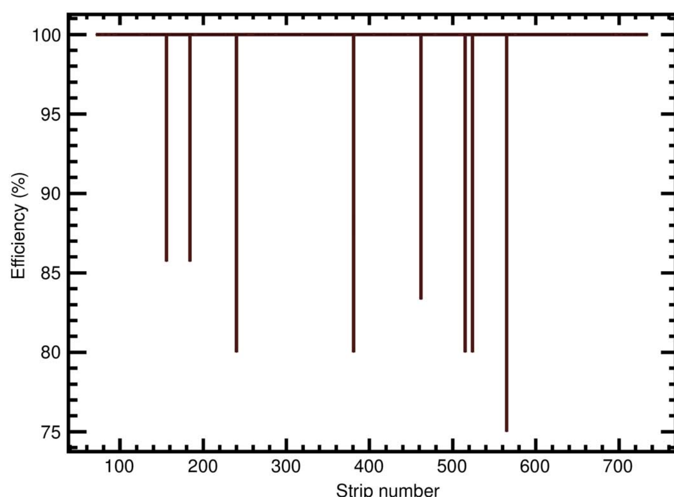


Fig. 11. The tracking efficiency as a function of the strip number.

signal distributions of MCz-Si (DUT) and one reference plane, showing highest signal among the eight planes. The data was recorded during the same data taking session and both sensors were biased with 150 V. The temperature of the cold box during the data taking was set to $-20^{\circ}$C.

The most probable values (MPV) of signal are 45 ADC and 41 ADC for DUT and reference sensors, respectively. The larger signal from the DUT is expected due to an approximately 10% higher effective thickness compared with the reference detector (315 $\mu$m vs. 290 $\mu$m). The strip noise distribution of DUT recorded during the same data taking run is presented in Fig. 10. The result is well in line with the expectations obtained from our previous studies using the very same setup, presented e.g. in Ref. [39].

The MPV of the noise distribution is 1.1 ADC counts, which would result in a signal-to-noise (SNR) ratio of about 41. Typical noise in reference planes is about 1.5 ADC. The noise seen in the MCz-Si DUT and the reference planes is, however, not directly comparable due to the different strip lengths. The resolution of the DUT was extracted from 35 data taking runs with different bias voltages 120-350 V. The resolution at the depletion voltage is $12\ \mu$m that is slightly below the digital resolution, i.e. $50\ \mu\mathrm{m}/\sqrt{12} = 14.4\ \mu$m for a $50\ \mu$m pitch sensor in case all the charge is collected in a single strip.

The global tracking efficiency of 99.6% was determined by the off-line data analysis. In other words, in average the MCz-Si detector missed about four events out of the one thousand events the tracks of which were found by the eight reference planes. This uniformity of the process over the 768 strips of the detector is illustrated in Fig. 11. As seen in the plot, there were only eight strips out of 564 measured strips, which performed with rather low efficiency.

## V. Conclusion

A set of strip sensors was made on 6-inch diameter high-resistivity MCz-Si wafers by using industrially feasible, largely automated and robust processing. The pre-processing material quality characterization shows very good homogeneity in terms of resistivity, oxygen concentration, and minority carrier lifetime. This is achieved by applying a magnetic field during the Czocharalski method crystal growth. Mechanical perturbations and oscillations in the molten silicon can be controlled by a magnetic field, which allows better tuning of the concentration of the oxygen and dopant impurities dissolving from the crucible. The full depletion voltage, extracted from C-V data, was found to be in range of 120-140 V in all devices produced in this batch. This corresponds to an effective resistivity of about $2.5-2.8$ kOhm·cm of phosphorous doped n-type MCz-Si material. For comparison, in our earlier studies we have used MCz-Si material with resistivities ranging from $0.9 - 1.1$ kOhm $\cdot$ cm with corresponding $\mathrm{V_{fd}}$ of about 300-350 V [9], [24], [27]. The leakage current density was less than $25$ nA/cm$^2$ measured from different size sensors at 200 V bias, i.e., clearly above the full depletion voltage. This is due to the high minority carrier lifetime ($> 3$ ms) that was maintained during the whole processing cycle.

The concentration of interstitial oxygen was found to be homogeneous and in the range of $2.9 - 3.0 \times 10^{17}$ cm$^{-3}$, which is slightly less than $5.0 \times 10^{17}$ cm$^{-3}$, reported earlier from MCz-Si material originating from different crystal [42]. It should be noted that MCz-Si materials used for particle detector applications have intentionally lower oxygen concentration than typically found in Czochralski method grown silicon used by microelectronics industry. During the processing, special care was taken to avoid the temperature range associated with the formation of thermal donors.

The presence of hydrogen has earlier been speculated to enhance the TD formation [43]. Hydrogen was present in large quantity in our process during e.g. polysilicon deposition from silane ($\mathrm{Si_3H_4}$), PECVD passivation layer deposition and during the sintering in forming gas. Nevertheless, our detector property measurements do not rule in or rule out the influence of hydrogen during the sensor processing.

The beam test results show that the MCz-Si sensor has performance comparable with commercially mass produced strip sensors delivered earlier for a large-scale particle physics experiment. The signal-to-noise ratio of MCz-Si sensors exceeds 40 when biased with 150 V, i.e., the same operating voltage that

was applied to the Fz-Si reference sensors. The noise performance of MCz-Si DUT and reference sensors, with 2.5 times longer strips, are not directly comparable, because the noise in our test beam setup is largely dominated by strip capacitance. The design of the sensors is very robust, 3.8 cm long strips with 50 and 80 $\mu$m pitches surrounded by a simple guard-ring structure. The choice of these strip parameters is mainly due to the foreseen fivefold luminosity in the HL-LHC, which consequently results in undesirable channel occupancy. For instance, in the current CMS experiment the strip sensors with lowest granularity have strip length of 20 cm (two daisy chained large sensors) and 240 $\mu$m pitch [37]. The resolution of MCz-Si DUT sensor is very close to the digital/binary resolution of the given segmentation. In unirradiated sensors, more than 90% of the signal charge is collected by the channel closest to the impact point, i.e. the charge sharing between the channels is almost negligible. In the high-luminosity environment, the resolution improvement by utilization of charge sharing between the channels is, however, largely limited because of the trapping by radiation defects. Taking into account the drift velocity saturation in the electric field, the effective charge collection distance will be in the order of strip pitch within given trapping time constant.

The CCE is a complex product of the electric field distribution E(x) and trapping in the heavily irradiated silicon. According to the existing knowledge, the trapping is largely independent of the silicon material properties. Thus, the way to improve the radiation-hardness is to optimize E(x), for instance a high electric field on the electrodes can be achieved with p-type detectors or thinner sensors. And elevating the oxygen concentration has also been one of the most successful methods to date. The essential difference between the MCz-Si and Fz-Si is the oxygen concentration. It is possible to enhance the oxygen concentration in Fz-Si by prolonged high temperature oxygen diffusion, which might last up to hundreds of hours. The compromise is, however, increased processing costs, limited number of qualified processing vendors as well as the risk of induced contamination. In summary, strip detectors made of 6-inch diameter high-resistivity MCz-Si wafers stand as mass production feasible and cost-effective candidate for future HEP experiments requiring ultimate radiation hardness.

## Acknowledgment

The authors are most grateful for I. McGill for the wire bonding of the MCz-Si sensor to the read-out hybrid at the CERN bonding laboratory and to H. Pohjonen for the chip dicing at VTT.

## References

[1] F. Gianotti, M. L. Mangano, T. Virdee, S. Abdullin, G. Azuelos, and A. Ball *et al.*, "Physics potential and experimental challenges of the LHC luminosity upgrade," *Eur. Phys. J.*, vol. C39, pp. 293–333, 2005.

[2] P. Allport and M. Nessi, "Letter of intent for the phase-I upgrade of the ALAS experiment," CERN-LHCC-2011-012; LHCC-I-020, Nov. 2011.

[3] J. Nash and A. Ball, "Technical proposal for the upgrade of the CMS detector through 2010," CERN-LHCC-2011-006; CMS-HG-TP-1; LHCC-P-004, Jun. 2011.

[4] G. Casse, "Overview of the recent activities of the RD50 collaboration on radiation hardening of semiconductor detectors for the sLHC," *Nucl. Instrum. Meth. A*, vol. 598, pp. 54–60, 2009.

[5] E. Fretwurst, J. Adey, A. Al-Ajili, G. Alfieri, P. P. Allport, and M. Artuso *et al.*, "Recent advancements in the development of radiation hard semiconductor detectors for S-LHC," *Nucl. Instrum. Meth. A*, vol. 552, pp. 7–19, 2005.

[6] S. Seidel, "Silicon detector for the super LHC," *Nucl. Instrum. Meth. A*, vol. 628, pp. 272–275, 2011.

[7] A. Dierlamm, "Characterization of silicon sensor materials and designs for the CMS tracker upgrade," *Pos (Vertex '12)*, vol. 016, 2012.

[8] G. Lindstroem, M. Ahmed, S. Albergo, P. Allport, D. Anderson, and L. Andricek *et al.*, "Developments for radiation hard silicon detectors by defect engineering—results by the CERN RD48 (ROSE) Collaboration," *Nucl. Instrum. Meth. A*, vol. 465, pp. 60–69, 2001.

[9] J. Härkönen, E. Tuominen, E. Tuovinen, P. Heikkilä, V. Ovchinnikov, and M. Yli-Koski *et al.*, "Processing microstrip detectors on Czochralski grown high resistivity silicon," *Nucl. Instrum. Meth. A*, vol. 514, pp. 173–179, 2003.

[10] Z. Li, J. Härkönen, W. Chen, J. Kierstead, P. Luukka, and E. Tuominen *et al.*, "Radiation hardness of high resistivity magnetic Czochralski silicon detectors after gamma, neutron, and proton radiations," *IEEE Trans. Nucl. Sci.*, vol. 51, no. 4, pp. 1901–1908, Aug. 2004.

[11] G. Casse, P. P. Allport, T. J. V. Bowcock, A. Greenall, M. Hanlon, and J. N. Jackson, "First results on the charge collection properties of segmented detectors made with p-type bulk silicon," *Nucl. Instrum. Meth. A*, vol. 487, pp. 460–470, 2002.

[12] Y. Unno, A. A. Affolder, P. P. Allport, R. Bates, C. Betancourt, and J. Bohm *et al.*, "Development of n-on-p silicon sensors for very high radiation environments," *Nucl. Instrum. Meth. A*, vol. 636, pp. 24–30, 2011.

[13] P. P. Allport, G. Casse, and A. Greenall, "Radiation tolerance of oxygenated n-strip read-out detectors," *Nucl. Instrum. Meth. A*, vol. 513, pp. 84–88, 2003.

[14] G. Kramberger and D. Contarato, "How to achieve highest charge collection efficiency in heavily irradiated position-sensitive silicon detector," *Nucl. Instrum. Meth. A*, vol. 560, pp. 98–102, 2006.

[15] S. Ramo, "Currents Induced by electron motion," *Proc. IRE*, vol. 27, no. 9, pp. 584–585, Sep. 1939.

[16] G. Pellegrini, C. Fleta, F. Campabadal, S. Díez, M. Lozano, and J. M. Rafí *et al.*, "Technology development of p-type microstrip detectors with radiation hard p-spray isolation," *Nucl. Instrum. Meth. A*, vol. 566, pp. 360–365, 2006.

[17] M. Bruzzi, D. Bisello, L. Borrello, E. Borchi, M. Boscardin, and A. Candelori *et al.*, "Processing and first characterization of detectors made with high resistivity n- and p-type Czochralski silicon," *Nucl. Instrum. Meth. A*, vol. 552, pp. 20–26, 2005.

[18] A. Affolder, P. Allport, and G. Casse, "Charge collection efficiencies of planar silicon detector after reactor neutron and proton doses up to $1.6 \times 10^{16} \mathrm{n_{eq}cm^{-2}}$," *Nucl. Instrum. Methods A*, vol. 612, pp. 470–473, 2010.

[19] A. Affolder, P. Allport, and G. Casse, "Collected charge of planar silicon detectors after pion and proton irradiations up to $2.2 \times 10^{16} \mathrm{n_{eq}\ cm^{-2}}$," *Nucl. Instrum. Methods A*, vol. 623, pp. 177–179, 2010.

[20] H. W. Kraner, Z. Li, and E. Fretwurst, "The use of the signal current pulse shape to study the internal electric field profile and trapping effects in neutron damaged silicon detectors," *Nucl. Instrum. Meth. A*, vol. 326, pp. 350–356, 1993.

[21] V. Eremin and Z. Li, "Determination of the Fermi level position for neutron irradiated high resistivity silicon detectors and materials using the Transient Charge Technique(TChT)," *IEEE Trans. Nucl. Sci.*, vol. 41, no. 6, pp. 1907–1912, Dec. 1994.

[22] V. Eremin, N. Strokan, E. Verbitskaya, and Z. Li, "Development of transient current and charge techniques for the measurement of effective net concentration of ionized charges (Neff) in the space charge region of p-n junction detectors," *Nucl. Instrum. Meth. A*, vol. 372, pp. 388–398, 1996.

[23] E. Tuovinen, J. Härkönen, P. Liikka, E. Tuominen, E. Verbitskaya, and V. Eremin *et al.*, "Czochralski silicon detectors irradiated with 24 GeV/c and 10 MeV protons," *Nucl. Instrum. Meth. A*, vol. 568, pp. 83–88, 2006.

[24] L. Spiegel, T. Barvich, B. Betchart, S. Bhattacharya, S. Czellar, and R. Demina *et al.*, "Czochralski silicon as a detector material for S-LHC tracker volumes," *Nucl. Instrum. Meth. A*, vol. 628, pp. 242–245, 2011.

[25] V. Eremin, Z. Li, S. Roe, G. Ruggiero, and E. Verbitskaya, "Double peak electric field distortion in heavily irradiated silicon strip detectors," *Nucl. Instrum. Meth. A*, vol. 535, pp. 622–631, 2004.

[26] P. Luukka, J. Härkönen, T. Mäenpää, B. Betchart, S. Czellar, and R. Demina *et al.*, "TCT and test beam results of irradiated magnetic Czochralski silicon (MCz-Si) detectors," *Nucl. Instrum. Meth. A*, vol. 604, pp. 254–257, 2009.

[27] E. Tuovinen, J. Härkönen, P. Luukka, T. Mäenpää, H. Moilanen, and I. Kassamakov *et al.*, "Magnetic Czochralski silicon strip detectors for Super-LHC experiments," *Nucl. Instrum. Meth. A*, vol. 636, pp. 79–82, 2011.

[28] *ASTM F 1188-93a: Standard Test Method for Interstitial Atomic Oxygen Content of Silicon by Infrared Absorption*, ASTM F 1188-93a, ASTM International, West Conshohocken, PA, USA, 1993.

[29] D. K. Schroder, "Semiconductor material and device characterization," in , 2nd ed. ed. New York, NY, USA: Wiley, 1998, pp. 429–437.

[30] J. Härkönen, E. Tuovinen, Z. Li, P. Luukka, E. Verbitskaya, and V. Eremin, "Recombination lifetime characterization and mapping of silicon wafers and detectors using the microwave photoconductivity decay ($\mu$PCD) technique," *Mat. Sci. Semicon. Proc.*, vol. 9, pp. 261–265, 2006.

[31] G. S. Oehrlein, "Silicon-oxygen complexes containing three oxygen atoms as the dominant thermal donor species in heat-treated oxygen-containing silicon," *J. Appl. Phys.*, vol. 54, pp. 5453–5455, 1983.

[32] K. Wada, "Unified model for formation kinetics of oxygen thermal donors in silicon," *Phys. Rev. B*, vol. 10, pp. 5884–5895, 1984.

[33] M. Bruzzi, J. Härkönen, Z. Li, P. Liikka, D. Menichelli, and E. Tuovinen *et al.*, "Thermal donor generation in Czochralski silicon particle detectors," *Nucl. Instrum. Meth. A*, vol. 568, pp. 56–60, 2006.

[34] M. Bruzzi, D. Menichelli, M. Scaringella, J. Härkönen, E. Tuovinen, and Z. Li, "Thermal donoros formation via isothermal annealing in magnetic Czochralski high resistivity silicon," *J. Appl. Phys.*, vol. 99, p. 093706, 2006.

[35] J. Härkönen, E. Tuovinen, P. Luukka, M. Moll, A. Bates, and Z. Li, "Proton irradiation results of $p+/n-/n+$ Cz-Si detectors processed on boron doped substrates with thermal donor induced space charge sign inversion," *Nucl. Instrum. Meth. A*, vol. 552, pp. 43–48, 2005.

[36] E. Tuovinen, J. Härkönen, P. Luukka, and E. Tuominen, "Intentional thermal donor activation in magnetic Czochralski silicon," *Mater. Sci. Semicond. Process.*, vol. 10, pp. 179–184, 2007.

[37] The CMS CollaborationR. Adolphi *et al.*, "The CMS experiment at the CERN LHC," JINST vol. 3, p. S08004, 2008.

[38] T. Mäenpää, P. Luukka, B. Betchart, S. Czellar, R. Demina, and Y. Gotra *et al.*, "Silicon beam telescope for LHC upgrade tests," *Nucl. Instrum. Meth. A*, vol. 593, pp. 523–529, 2008.

[39] P. Luukka, E. Tuominen, S. Korjenevski, T. Mäenpää, H. Viljanen, and R. Demina *et al.*, "Test beam results of heavily irradiated magnetic Czochralski silicon (MCz-Si) strip detectors," *Nucl. Instrum. Meth. A*, vol. 612, pp. 497–500, 2010.

[40] M. Demarteau, R. Demina, S. Korjenevski, F. Lehner, R. Lipton, and H. S. Mao *et al.*, "Characteristics of the outer layer silicon sensors for the Run IIb silicon detector," *D0 note 4308*, Mar. 4, 2003.

[41] T. Mäenpää, M. J. Kortelainen, and T. Lampén, "Track-Induced clustering in position sensitive detector characterization," *IEEE Trans. Nucl. Sci.*, vol. 57, no. 4, pp. 2196–2199, Aug. 2010.

[42] J. Härkönen, E. Tuovinen, P. Luukka, H. K. Nordlund, and E. Tuominen, "Magnetic Czochralski silicon as detector material," *Nucl. Instrum. Meth. A*, vol. 579, pp. 648–652, 2007.

[43] A. Simoen, C. Claeys, R. Job, A. G. Ulyashin, W. R. Fahrner, and O. De Gryse *et al.*, "Hydrogen plasma-enhanced thermal donor formation in n-type oxygendoped high-resistivity float-zone silicon," *Appl. Phys. Lett.*, vol. 81, p. 1842, 2002.